

## A Challenge to Chemical Intuition: Donor–Acceptor Interactions in $\text{H}_3\text{B–L}$ and $\text{H}_2\text{B}^+–\text{L}$ ( $\text{L} = \text{CO}; \text{EC}_5\text{H}_5$ , $\text{E} = \text{N–Bi}$ )

Stefan Erhardt<sup>[a, b]</sup> and Gernot Frenking<sup>\*[b]</sup>

**Abstract:** The equilibrium geometries and bond energies of the complexes  $\text{H}_3\text{B–L}$  and  $\text{H}_2\text{B}^+–\text{L}$  ( $\text{L} = \text{CO}; \text{EC}_5\text{H}_5$ ;  $\text{E} = \text{N, P, As, Sb, Bi}$ ) have been calculated at the BP86/TZ2P level of theory. The nature of the donor–acceptor bonds was investigated by energy decomposition analysis (EDA). The bond strengths of  $\text{H}_3\text{B–L}$  have the order  $\text{CO} > \text{N} > \text{P} > \text{As} > \text{Sb} > \text{Bi}$ . The calculated values are between  $D_e = 37.1 \text{ kcal mol}^{-1}$  for  $\text{H}_3\text{B–CO}$  and  $D_e = 6.9 \text{ kcal mol}^{-1}$  for  $\text{H}_3\text{B–BiC}_5\text{H}_5$ . The bond dissociation energies of the cations  $\text{H}_2\text{B}^+–\text{CO}$  and  $\text{H}_2\text{B}^+–\text{EC}_5\text{H}_5$  are larger than for  $\text{H}_3\text{B–L}$ , particularly for complexes of the heterobenzene ligands. The calculated values are between  $D_e = 51.9 \text{ kcal mol}^{-1}$  for  $\text{H}_2\text{B}^+–\text{CO}$  and  $D_e = 122.1 \text{ kcal mol}^{-1}$  for  $\text{H}_2\text{B}^+–\text{NC}_5\text{H}_5$ . The trend of the BDE of  $\text{H}_2\text{B}^+–\text{CO}$  and  $\text{H}_2\text{B}^+–\text{EC}_5\text{H}_5$  is  $\text{N} > \text{P} > \text{As} > \text{Sb} > \text{Bi} > \text{CO}$ . A surprising result is found for  $\text{H}_2\text{B}^+–\text{CO}$ , which

has a significantly stronger and yet substantially longer bond than  $\text{H}_3\text{B–CO}$ . The reason for the longer but stronger bond in  $\text{H}_2\text{B}^+–\text{CO}$  compared with that in  $\text{H}_3\text{B–CO}$  comes mainly from the change in electrostatic attraction and  $\pi$  bonding at shorter distances, which increases more in the neutral system than in the cation, and to a lesser extent from the deformation energy of the fragments. The  $\text{H}_2\text{B}^+–\text{NC}_5\text{H}_5$   $\pi_{\perp}$  donation plays an important role for the stronger interactions at shorter distances compared with those in  $\text{H}_3\text{B–NC}_5\text{H}_5$ . The attractive interaction in  $\text{H}_2\text{B}^+–\text{CO}$  further increases at bond lengths that are shorter than the equilibrium value, but this is compensated

by the energy which is necessary to deform  $\text{BH}_2^+$  from its linear equilibrium geometry to the bent form in the complex. The EDA shows that the contributions of the orbital interactions to the donor–acceptor bonds are always larger than the classical electrostatic contributions, but the latter term plays an important role for the trend in bond strength. The largest contributions to the orbital interactions come from the  $\sigma$  orbitals. The EDA calculations suggest that heterobenzene ligands may become moderately strong  $\pi$  donors in complexes with strong Lewis acids, while CO is only a weak  $\pi$  donor. The much stronger interaction energies in  $\text{H}_2\text{B}^+–\text{EC}_5\text{H}_5$  compared with those in  $\text{H}_3\text{B–EC}_5\text{H}_5$  are caused by the significantly larger contribution of the  $\pi_{\perp}$  orbitals in  $\text{H}_2\text{B}^+–\text{EC}_5\text{H}_5$  and by the increase of the binding interactions of the  $\sigma + \pi_{\parallel}$  orbitals.

**Keywords:** bond energy • bond theory • density functional calculations • donor–acceptor systems • energy decomposition analysis

### Introduction

Chemical bonding between a Lewis acid and a Lewis base is usually described in terms of donor–acceptor interactions between the occupied orbitals of the donor and the vacant orbitals of the acceptor. The generally accepted bonding

model, first suggested by Dewar<sup>[1]</sup> and later elaborated by Chatt and Duncanson,<sup>[2]</sup> focuses on donor→acceptor  $\sigma$  donation and acceptor→donor  $\pi$  backdonation.<sup>[3]</sup> Figure 1 shows as a typical example for the Dewar–Chatt–Duncanson (DCD) model of the orbital interactions between a main-group Lewis acid A and CO as a Lewis base. An often neglected component is the donor→acceptor  $\pi$  donation which may occur from the degenerate occupied CO  $\pi$  orbital into a vacant  $\pi^*$  orbital of the Lewis acid (Figure 1c).<sup>[4]</sup>

We recently carried out a systematic theoretical study of the donor–acceptor interactions in complexes with heterobenzene ligands  $\text{EC}_5\text{H}_5$  ( $\text{E} = \text{N–Bi}$ ), which can serve as six-electron donors through the  $\pi$  electrons or as two-electron donors via the electron lone-pair of E.<sup>[5]</sup> The orbital interactions of the latter are schematically shown in Figure 2.

[a] Dr. S. Erhardt

School of EPS - Chemistry, Perkin Building (2.32)  
Heriot-Watt University, Edinburgh EH14 4AS (UK)

[b] Dr. S. Erhardt, Prof. G. Frenking

Fachbereich Chemie, Philipps-Universität Marburg  
Hans-Meerwein-Strasse, 35043 Marburg (Germany)  
Fax: (+49) 6421-282-5566  
E-mail: Frenking@chemie.uni-marburg.de

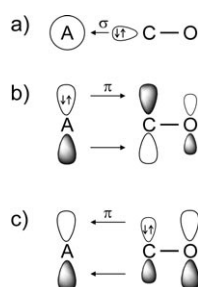


Figure 1. Schematic representation of the most important orbital interactions between CO as donor and a main-group Lewis acid A as acceptor. a)  $\text{CO} \rightarrow \text{A}$   $\sigma$  donation. b)  $\text{A} \rightarrow \text{CO}$   $\pi$  backdonation. c)  $\text{CO} \rightarrow \text{A}$   $\pi$  donation.

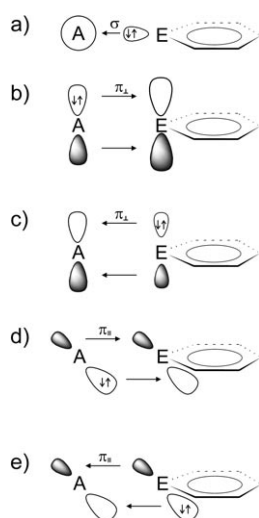


Figure 2. Schematic representation of the most important orbital interactions between heterobenzenes  $\text{EC}_5\text{H}_5$  as donor and a main-group Lewis acid A as acceptor. a)  $\text{EC}_5\text{H}_5 \rightarrow \text{A}$   $\sigma$  donation. b)  $\text{A} \rightarrow \text{EC}_5\text{H}_5$   $\pi_{\perp}$  backdonation. c)  $\text{EC}_5\text{H}_5 \rightarrow \text{A}$   $\pi_{\perp}$  donation. d)  $\text{A} \rightarrow \text{EC}_5\text{H}_5$   $\pi_{\parallel}$  backdonation. e)  $\text{EC}_5\text{H}_5 \rightarrow \text{A}$   $\pi_{\parallel}$  donation. Note that the out-of-plane  $p(\pi_{\perp})$  orbital of E represents the  $\pi_{\perp}$  orbitals of the ring. Also, the in-plane  $p(\pi_{\parallel})$  orbital of E represents the  $\pi_{\parallel}$  orbitals of the ring. The  $\pi_{\perp}$  orbitals are defined as orbitals that are antisymmetric with respect to the mirror plane which lies in the ring plane. The  $\pi_{\parallel}$  orbitals are defined as orbitals that are antisymmetric with respect to the mirror plane which bisects the ring plane.

Clearly,  $\text{EC}_5\text{H}_5$  can also in principle serve as a  $\pi$  donor (Figure 2c), besides the familiar  $\sigma$  donation and  $\pi$  backdonation (Figure 2a and b). One difference between the ligands CO and  $\text{EC}_5\text{H}_5$  is that the  $\pi$  orbitals in the former are degenerate, while in the latter they are split into out-of-plane ( $\pi_{\perp}$ ) and in-plane ( $\pi_{\parallel}$ ) orbitals. Donation and backdonation of the  $\pi_{\perp}$  and  $\pi_{\parallel}$  orbitals are shown in Figure 2b–e. Note that the  $p(\pi)$  AO of E stands for the ring orbitals of  $\text{EC}_5\text{H}_5$ . We were interested in the  $\pi$ -donor strength and a comparison of heterobenzene ligands  $\text{EC}_5\text{H}_5$  with CO. To this end we calculated the complexes of  $\text{EC}_5\text{H}_5$  and CO with the Lewis acids  $\text{BH}_3$  and  $\text{BH}_2^+$ .  $\text{BH}_2^+$  was chosen because it has no occupied out-of-plane  $\pi_{\perp}$  orbital. The calculated energy contributions of the  $\pi_{\perp}$  orbital interactions are therefore a direct estimate of the  $\pi$ -donor strength of  $\text{EC}_5\text{H}_5$  and CO.

We investigated the nature of the donor–acceptor interactions with the energy decomposition analysis (EDA) of the

program  $\text{ADF}^{[6]}$  which is based on the methods developed by Ziegler and Rauk<sup>[7]</sup> and Morokuma and Kitaura.<sup>[8]</sup> The EDA has successfully been used by us in systematic studies of donor–acceptor complexes.<sup>[9]</sup> The advantage of EDA is that the donor–acceptor bonding is analyzed not only in terms of orbital interactions but also in terms of quasiclassical electrostatic interaction. The two components, that is, orbital interactions and electrostatic attraction, are the two poles of the hard and soft acids and bases (HSAB) model introduced by Pearson.<sup>[10]</sup> A third component of the total donor–acceptor interaction is the Pauli repulsion between electrons having the same spin. The Pauli repulsion is the force which is considered as the main factor in the valence-shell electron pair repulsion (VSEPR) model of Gillespie et al.<sup>[11]</sup> The EDA is thus a method which encompasses all factors that are considered in the DCD, HSAB, and VSEPR models. Here we report on surprising results which challenge chemical intuition.

## Methods

The geometries of the molecules were optimized at the non-local DFT level of theory by using the exchange functional of Becke<sup>[12]</sup> in conjunction with the correlation functional of Perdew<sup>[13]</sup> (BP86). Uncontracted Slater-type orbitals (STOs) were employed as basis functions for the SCF calculations.<sup>[14]</sup> The basis sets have triple- $\zeta$  quality augmented by two sets of polarization functions, that is, p and d functions on hydrogen and d and f functions on the other atoms. This level of theory is denoted BP86/TZ2P. An auxiliary set of s, p, d, f, and g STOs was used to fit the molecular densities and to represent the Coulomb and exchange potentials accurately in each SCF cycle.<sup>[15]</sup> Scalar relativistic effects were considered by using the zero-order regular approximation (ZORA).<sup>[16]</sup> All structures were verified as minima on the potential energy surface by calculating the Hessian matrices. The partial charges were calculated with the Hirshfeld partitioning scheme.<sup>[17]</sup> The calculations were carried out with the program package  $\text{ADF}(2.3)$ .<sup>[18]</sup>

The  $\text{H}_3\text{B}-\text{L}$  and  $\text{H}_2\text{B}^+-\text{L}$  ( $\text{L} = \text{CO}$ ,  $\text{EC}_5\text{H}_5$ ) donor–acceptor interactions were analyzed by means of the energy partitioning scheme of  $\text{ADF}^{[6]}$ . The focus of the bonding analysis is the instantaneous interaction energy  $\Delta E_{\text{int}}$  of the bond, which is the energy difference between the molecule and the fragments in the frozen geometry of the compound. The interaction energy can be divided into three main components [Eq. (1)]:

$$\Delta E_{\text{int}} = \Delta E_{\text{elstat}} + \Delta E_{\text{Pauli}} + \Delta E_{\text{orb}} \quad (1)$$

where  $\Delta E_{\text{elstat}}$  is the electrostatic interaction energy between the fragments, which are calculated by using the frozen electron density distribution of the fragments  $\text{H}_3\text{B}$ ,  $\text{H}_2\text{B}^+$ , CO,  $\text{EC}_5\text{H}_5$  in the geometry of the molecules  $\text{H}_3\text{B}-\text{L}$  and  $\text{H}_2\text{B}^+-\text{L}$ .  $\Delta E_{\text{Pauli}}$  refers to the repulsive interactions between the

fragments, which are caused by the fact that two electrons with the same spin cannot occupy the same region in space.  $\Delta E_{\text{Pauli}}$  is calculated by enforcing the Kohn–Sham determinant on the superimposed fragments to obey the Pauli principle by antisymmetrization and renormalization. The stabilizing orbital interaction term  $\Delta E_{\text{orb}}$  is calculated in the final step of the energy partitioning analysis when the Kohn–Sham orbitals relax to their optimal form. This term can be further partitioned into contributions by the orbitals belonging to different irreducible representations of the point group of the interacting system. Note that the  $\Delta E_{\text{orb}}$  term includes also effects of polarization which come from the electrostatic interactions yielding deformation of the charge distribution without genuine orbital interactions taking place. Previous studies have shown that the contribution of the polarization term is rather small.<sup>[31d]</sup> The interaction energy  $\Delta E_{\text{int}}$  can be used to calculate the bond dissociation energy  $D_e$  by adding  $\Delta E_{\text{prep}}$ , which is the energy necessary to promote the fragments from their equilibrium geometry to the geometry in the compounds [Eq. (2)] Further details of the energy partitioning analysis can be found in the literature.<sup>[6]</sup>

$$-D_e = \Delta E_{\text{prep}} + \Delta E_{\text{int}} \quad (2)$$

The geometries of  $\text{H}_3\text{B}-\text{CO}$  and  $\text{H}_2\text{B}^+-\text{CO}$  were also optimized at the QCISD level<sup>[19]</sup> with a 6-311G(d,p) basis set.<sup>[20]</sup> The bond energies were then calculated by the CBS-QB3 method of Petersson et al.<sup>[21]</sup> The latter calculations were carried out with the program package Gaussian 03.<sup>[22]</sup>

## Results and Discussion

### Geometries and bond dissociation energies:

The geometry optimization of  $\text{H}_3\text{B}-\text{CO}$  gave the expected  $C_{3v}$ -symmetric structure, while the equilibrium structures of  $\text{H}_3\text{B}-\text{EC}_5\text{H}_5$  have  $C_s$  symmetry, as schematically shown in Figure 3 a. Table 1 lists the most important bond lengths and angles and the bond dissociation energies of the complexes. The calculated value for the  $\text{H}_3\text{B}-\text{CO}$  bond length at the BP86/TZ2P level (1.508 Å) is slightly shorter than the experimental value (1.534 ± 0.01 Å)<sup>[23]</sup> while the QCISD(T)/6-311G(d,p) value (1.577 Å) is a bit too long. The lowest lying conformation of the  $\text{BH}_3$  moiety in  $\text{H}_3\text{B}-\text{EC}_5\text{H}_5$  has one B–H bond orthogonal

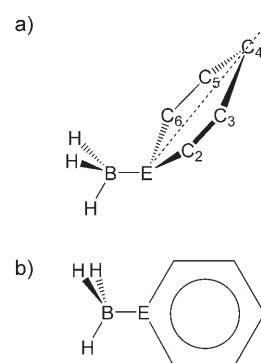


Figure 3. Schematic representation of the optimized geometries of complexes  $\text{H}_3\text{B}-\text{EC}_5\text{H}_5$ . a) Equilibrium geometry ( $C_s$ ). b) Symmetry-constrained ( $C_s$ ) structure which was used for the EDA calculations. In the latter structure the mirror plane of the ring moiety  $\text{EC}_5\text{H}_5$  is also the mirror plane of the complex  $\text{H}_3\text{B}-\text{EC}_5\text{H}_5$ . Note that the angle B–E–C4 in the equilibrium geometry is nearly 180° for E = N, P, As, Sb (Table 1).

to the ring plane. The B–E–C4 angle is slightly less than 180° except for  $\text{H}_3\text{B}-\text{BiC}_5\text{H}_5$ , which has a more acute angle of 136.3°. Thus, the mirror plane of the  $C_s$  equilibrium structures of  $\text{H}_3\text{B}-\text{EC}_5\text{H}_5$  bisects the ring plane of the  $\text{EC}_5\text{H}_5$  moiety. This is important for the orbital interaction analysis given below.

The theoretically predicted values for the bond dissociation energy (BDE) of the neutral compounds  $\text{H}_3\text{B}-\text{L}$  have the order  $\text{L} = \text{CO} > \text{N} > \text{P} > \text{As} > \text{Sb} > \text{Bi}$ , where the atomic symbols stand for the heteroarenes. A comparison with experimental results and previous theoretical studies indicates that the BP86/TZ2P value for  $\text{H}_3\text{B}-\text{CO}$  ( $D_0 = 34.0 \text{ kcal mol}^{-1}$ ) is too large. Experimental heats of formation of the

Table 1. Calculated and experimental bond lengths [Å], bond angles [°], and bond dissociation energies  $D_e$  and  $D_0$  [kcal mol<sup>-1</sup>] of  $\text{H}_3\text{B}-\text{CO}$ ,  $\text{H}_3\text{B}-\text{EC}_5\text{H}_5$ ,  $\text{H}_2\text{B}^+-\text{CO}$ , and  $\text{H}_2\text{B}^+-\text{EC}_5\text{H}_5$  (E = N, P, As, Sb, Bi) at the BP86/TZ2P level. Experimental values are given in parentheses. The calculated values for  $\text{H}_3\text{B}-\text{CO}$  and  $\text{H}_2\text{B}^+-\text{CO}$  at the CBS/QB3//QCISD(T)/6-311G(d,p) level are given in italics.

	CO	N	P	As	Sb	Bi
$\text{H}_3\text{B}-\text{CO}, \text{H}_3\text{B}-\text{EC}_5\text{H}_5$						
B–E	1.508; 1.577 (1.534 ± 0.01) <sup>[a]</sup>	1.605	1.933	2.086	2.355	2.586
E–C2 (C–O)	1.143; <sup>[b]</sup> 1.130 <sup>[c]</sup> (1.135 ± 0.01) <sup>[a]</sup>	1.352	1.725	1.847	2.050	2.170
C2–C3		1.389	1.394	1.391	1.390	1.384
C3–C4		1.396	1.397	1.401	1.403	1.407
C2–E–C6		118.7	104.4	100.8	94.9	90.5
B–E–C4		177.9	178.7	178.8	178.2	136.3
$D_e$	37.1; 25.2	35.6; 36.1	25.8	16.6	12.1	6.9
$D_0$	34.0; 22.1 <sup>[d]</sup> (24.6) <sup>[e]</sup>	31.2; 31.7	22.4	15.2	12.5	6.6
$\text{H}_2\text{B}^+-\text{CO}, \text{H}_2\text{B}^+-\text{EC}_5\text{H}_5$						
B–E	1.611; 1.661	1.491	1.888	1.993	2.200	2.290
E–C2 (C–O)	1.122; <sup>[b]</sup> 1.117 <sup>[c]</sup>	1.373	1.725	1.845	2.044	2.142
C2–C3		1.380	1.388	1.385	1.384	1.379
C3–C4		1.400	1.405	1.407	1.409	1.409
C2–E–C6		120.0	108.7	104.8	98.6	95.3
$D_e$	51.9; 45.4	122.1; 119.3	94.7	83.6	75.8	65.4
$D_0$	49.0; 42.5 <sup>[d]</sup>	117.2; 114.4	91.2	81.8	74.8	64.8

[a] Experimental value.<sup>[23]</sup> [b] Calculated value for free CO: 1.136 Å. [c] Calculated value for free CO: 1.133 Å. [d] ZPE correction at BP86/TZ2P level. [e] Experimental value taken from the heats of formation.<sup>[24]</sup>

complex and the dissociation products<sup>[24]</sup> give a value of  $D_o = 24.6 \text{ kcal mol}^{-1}$  which is in good agreement with previous ab initio studies<sup>[25,26]</sup> at the MP2/TZ2P<sup>[27]</sup> ( $D_o = 23.0 \text{ kcal mol}^{-1}$ ) and CBS-4<sup>[21]</sup> levels ( $D_o = 21.9 \text{ kcal mol}^{-1}$ ). The latter work also gives a BDE for H<sub>3</sub>B–NC<sub>5</sub>H<sub>5</sub> ( $D_o = 32.0 \text{ kcal mol}^{-1}$ ) which is in excellent agreement with the BP86/TZ2P value reported here ( $D_o = 31.2 \text{ kcal mol}^{-1}$ , Table 1). It thus seems that BP86/TZ2P overestimates the bond energy of H<sub>3</sub>B–L for L=CO but not for L=EC<sub>5</sub>H<sub>5</sub>. Our calculated BDE values at the CBS/QB3 level for H<sub>3</sub>B–CO and H<sub>3</sub>B–NC<sub>5</sub>H<sub>5</sub> are in good agreement with previous results (Table 1).

Table 1 also lists the interatomic distances, bond angles, and bond dissociation energies of the planar ( $C_{2v}$ ) equilibrium structures of H<sub>2</sub>B<sup>+</sup>–CO and H<sub>2</sub>B<sup>+</sup>–EC<sub>5</sub>H<sub>5</sub>. A comparison of the calculated data for the neutral complexes with those of the cations shows some peculiar results. The bond energies of the H<sub>2</sub>B<sup>+</sup>–L complexes are as expected higher than the values for H<sub>3</sub>B–L, because positively charged BH<sub>2</sub><sup>+</sup> is a stronger Lewis acid than BH<sub>3</sub>. However, the increase is much larger when L=EC<sub>5</sub>H<sub>5</sub> than for L=CO, for which the bond energy increases only moderately. For example, the  $D_o$  value of the carbonyl complexes increases from 34.0 kcal mol<sup>-1</sup> in H<sub>3</sub>B–CO to 49.0 kcal mol<sup>-1</sup> in H<sub>2</sub>B<sup>+</sup>–CO, while the values for the pyridine complexes increase from 31.2 kcal mol<sup>-1</sup> in H<sub>3</sub>B–NC<sub>5</sub>H<sub>5</sub> to 117.2 kcal mol<sup>-1</sup> in H<sub>2</sub>B<sup>+</sup>–NC<sub>5</sub>H<sub>5</sub> (Table 1). The theoretically predicted bond energies of the H<sub>2</sub>B<sup>+</sup>–L complexes have the order N>P>As>Sb>Bi>CO, that is, CO is now the most weakly bonded ligand. This result does not change when the calculated bond energies at the CBS/QB3 level for H<sub>2</sub>B<sup>+</sup>–CO ( $D_o = 42.5 \text{ kcal mol}^{-1}$ ) and H<sub>2</sub>B<sup>+</sup>–NC<sub>5</sub>H<sub>5</sub> ( $D_o = 114.4 \text{ kcal mol}^{-1}$ ) are considered (Table 1). The results clearly show that it is not possible to establish a generally valid order for the strength of the Lewis basicity of nucleophilic species. The strength of the donor–acceptor interactions depends on the nature of the bond, and different Lewis acids may exhibit different orders of bond strength with a set of Lewis bases because the nature of the donor–acceptor interactions is not the same.

A second surprising result are the calculated H<sub>2</sub>B<sup>+</sup>–L bond lengths. The higher BDE of the charged complexes suggests that the donor–acceptor bonds should become

shorter in the cations than in the neutral compounds H<sub>3</sub>B–L. Table 1 shows that this is indeed the case when L=EC<sub>5</sub>H<sub>5</sub>. The B–E distances in H<sub>2</sub>B<sup>+</sup>–EC<sub>5</sub>H<sub>5</sub> are always significantly shorter than in H<sub>3</sub>B–EC<sub>5</sub>H<sub>5</sub>. This does not hold for L=CO, however. The calculated H<sub>2</sub>B<sup>+</sup>–CO bond is clearly longer (1.611 Å) than the H<sub>3</sub>B–CO bond (1.508 Å), although the former has a stronger bond than the latter. To rule out that this result is an artifact of the method we carried out ab initio calculations for H<sub>2</sub>B<sup>+</sup>–CO and H<sub>3</sub>B–CO at the CBS/QB3 level<sup>[21]</sup> using QCISD/6-311G(d,p) optimized geometries.<sup>[19]</sup> Table 1 shows that the ab initio calculations make the same prediction, that is, the H<sub>2</sub>B<sup>+</sup>–CO bond is longer (1.661 Å) but stronger ( $D_o = 42.5 \text{ kcal mol}^{-1}$ ) than the H<sub>3</sub>B–CO bond, which is shorter (1.577 Å) but weaker ( $D_o = 22.1 \text{ kcal mol}^{-1}$ ). Shorter but weaker donor–acceptor bonds have been reported before,<sup>[28]</sup> and it has been pointed out that bond lengths and bond strength do not necessarily correlate with each other, although this is generally assumed.<sup>[29]</sup> The present example is particularly striking and deserves to be analyzed in detail (see next section).

**Bonding analysis:** We investigated the nature of the donor–acceptor bonds in H<sub>3</sub>B–L and H<sub>2</sub>B<sup>+</sup>–L by energy decomposition analysis (EDA) in order to understand the peculiar results presented above. Table 2 lists the EDA results for H<sub>3</sub>B–CO and H<sub>3</sub>B–EC<sub>5</sub>H<sub>5</sub>. The EDA calculations on the former compound were carried out on the  $C_{3v}$  equilibrium geometry. The bonding analysis of H<sub>3</sub>B–EC<sub>5</sub>H<sub>5</sub> was performed not for the equilibrium geometries but for optimized structures with symmetry constraints as shown in Figure 3. The equilibrium structures (Figure 3a) and the distorted form (Figure 3b) both have  $C_s$  symmetry. The difference between the two forms is that the mirror plane of the former structure bisects the ring plane of the EC<sub>5</sub>H<sub>5</sub> moiety, while in the latter the ring plane lies in the mirror plane. This means that the a' orbitals of the H<sub>3</sub>B–EC<sub>5</sub>H<sub>5</sub> equilibrium structure have contributions coming from the  $\sigma$  and  $\pi_{\perp}$  orbitals of EC<sub>5</sub>H<sub>5</sub> while the a'' orbitals of the complex have contributions from the  $\pi_{\parallel}$  orbitals of EC<sub>5</sub>H<sub>5</sub>. The energy contributions of the  $\sigma$  and  $\pi_{\perp}$  EC<sub>5</sub>H<sub>5</sub> orbitals can therefore not be calculated separately. In the constrained structure (Figure 3b) the a' orbitals of the H<sub>3</sub>B–EC<sub>5</sub>H<sub>5</sub> equilibrium struc-

Table 2. EDA results [kcal mol<sup>-1</sup>] of H<sub>3</sub>B–CO and H<sub>3</sub>B–EC<sub>5</sub>H<sub>5</sub> (E=N, P, As, Sb, Bi) and partial charges  $q(\text{BH}_3)$  at the BP86/TZ2P level. H<sub>3</sub>B–EC<sub>5</sub>H<sub>5</sub> was analyzed with the  $C_s$  structure shown in Figure 3b.

Term	CO	N	P	As	Sb	Bi
$\Delta E_{\text{int}}$	-50.3	-51.1	-38.2	-26.1	-17.8	-9.3
$\Delta E_{\text{Pauli}}$	151.9	122.0	111.7	83.6	60.9	38.5
$\Delta E_{\text{elstat}}^{\text{[a]}}$	-73.9 (36.5%)	-86.5 (49.9%)	-57.4 (38.3%)	-39.6 (36.1%)	-27.3 (34.7%)	-15.8 (33.2%)
$\Delta E_{\text{orb}}^{\text{[a]}}$	-128.3 (63.5%)	-86.7 (50.1%)	-92.4 (61.7%)	-70.0 (63.9%)	-51.5 (65.3%)	-31.9 (66.8%)
a' ( $\sigma + \pi_{\parallel}$ ) <sup>[b]</sup>	-109.7 (85.5%)	-77.7 (89.6%)	-83.9 (90.7%)	-64.5 (92.1%)	-48.0 (93.3%)	-29.9 (93.7%)
a'' ( $\pi_{\perp}$ ) <sup>[b]</sup>	-18.6 (14.5%)	-9.0 (10.4%)	-8.6 (9.3%)	-5.5 (7.9%)	-3.4 (6.7%)	-2.0 (6.3%)
$\Delta E_{\text{prep}}$	13.2	15.6	12.5	9.4	5.7	2.4
$D_e$	37.1	35.6	25.8	16.6	12.1	6.9
$D_o$	33.9	31.7	23.4	14.5	10.2	5.4
$q(\text{BH}_3)$	0.08	-0.14	-0.08	-0.11	-0.12	-0.11

[a] The value in parentheses gives the percentage contribution to the total attractive interactions. [b] The symmetry notation in parentheses refers to the orbitals of the donor moiety. The value in parentheses gives the percentage contribution to the total orbital interactions.

ture have contributions from the  $\sigma$  and  $\pi_{\parallel}$  orbitals of  $\text{EC}_5\text{H}_5$ , while the  $a''$  orbitals of the complex have contributions from the  $\pi_{\perp}$  orbitals of  $\text{EC}_5\text{H}_5$ . Since the latter contribution is the focus of the orbital analysis (Figure 2), we used the structure shown in Figure 3b for the EDA calculations. The constrained structures of  $\text{H}_3\text{B}-\text{EC}_5\text{H}_5$  are only slightly higher in energy than the equilibrium structure. The calculated differences are less than  $0.1 \text{ kcal mol}^{-1}$  for  $\text{E}=\text{N}-\text{Sb}$  and  $0.41 \text{ kcal mol}^{-1}$  for  $\text{H}_3\text{B}-\text{BiC}_5\text{H}_5$ . We think that the energy differences are negligible for the EDA, which now yields the contribution of the  $\pi_{\perp}$  orbitals of the ligand to the  $\Delta E_{\text{orb}}$  term. To facilitate comparison, the EDA data of  $\text{H}_3\text{B}-\text{CO}$  in Table 2 are also given in  $C_s$  symmetry. Note that the contributions of the  $\pi_{\perp}$  and  $\pi_{\parallel}$  orbitals in  $\text{H}_3\text{B}-\text{CO}$  are the same, and therefore it is possible to calculate the  $\sigma$  and  $\pi$  interactions for this complex from the EDA data of the  $C_s$  structure.

The EDA shows that the largest contribution to the overall interaction energy  $\Delta E_{\text{int}}$  in all complexes  $\text{H}_3\text{B}-\text{L}$  comes from the repulsive term  $\Delta E_{\text{Pauli}}$ . The largest attractive contribution to the  $\text{H}_3\text{B}-\text{CO}$  bond comes from the orbital term  $\Delta E_{\text{orb}}$ , which provides 63.5% of the binding interactions, while the electrostatic attraction contributes 36.5%. The two terms  $\Delta E_{\text{orb}}$  and  $\Delta E_{\text{elstat}}$  are nearly equally strong in  $\text{H}_3\text{B}-\text{NC}_5\text{H}_5$ . The relative contribution of the  $\Delta E_{\text{orb}}$  term increases for the  $\text{H}_3\text{B}-\text{EC}_5\text{H}_5$  bond when E becomes heavier (Table 2). We note that a change in the classical electrostatic interactions has a significant influence on the trend of the  $\text{H}_3\text{B}-\text{L}$  bond strength. The  $\Delta E_{\text{elstat}}$  value in  $\text{H}_3\text{B}-\text{NC}_5\text{H}_5$  is larger ( $-86.5 \text{ kcal mol}^{-1}$ ) than that in  $\text{H}_3\text{B}-\text{CO}$  ( $-73.9 \text{ kcal mol}^{-1}$ ), although the former complex has a longer donor-acceptor bond than the latter. This can be explained with the more diffuse (greater p character) lone pair orbital of  $\text{NC}_5\text{H}_5$  compared to that of  $\text{CO}$ . The larger  $\Delta E_{\text{elstat}}$  value and the smaller Pauli repulsion of  $\text{H}_3\text{B}-\text{NC}_5\text{H}_5$  compensate for the clearly weaker orbital interactions ( $-86.7 \text{ kcal mol}^{-1}$ ) compared with  $\text{H}_3\text{B}-\text{CO}$  ( $-128.3 \text{ kcal mol}^{-1}$ ). Note that the  $\Delta E_{\text{elstat}}$  values of  $\text{H}_3\text{B}-\text{EC}_5\text{H}_5$  follow the same diminishing trend  $\text{N} > \text{P} > \text{As} > \text{Sb} > \text{Bi}$  as the total values for  $\Delta E_{\text{int}}$ , while  $\Delta E_{\text{orb}}$  first increases from N to P before it becomes smaller (Table 2).

Very interesting information comes from the breakdown of the  $\Delta E_{\text{orb}}$  term into contributions from orbitals having  $a'$  and  $a''$  symmetry. The former orbitals are the  $\sigma$  and  $\pi_{\parallel}$  orbitals (Figure 2a), while the latter are the  $\pi_{\perp}$  orbitals (Figure 2b) of the complex and the ligand. The EDA data in Table 2 show that the  $\Delta E_{\text{orb}}(a'')$  term of the complexes  $\text{H}_3\text{B}-\text{EC}_5\text{H}_5$  is not very large. It contributes only between 6.3 and 10.4% to the total orbital interactions. The contribution of the  $\Delta E_{\text{orb}}(a'')$  term in  $\text{H}_3\text{B}-\text{CO}$  is larger. In the latter compound, the  $\pi_{\perp}$  and  $\pi_{\parallel}$  orbitals are degenerate. Each component contributes 14.5% to the total orbital interactions, which means that the  $\pi$  orbitals in  $\text{H}_3\text{B}-\text{CO}$  yield 29.0% of the  $\Delta E_{\text{orb}}$  term. It remains open, however, how much of the  $\Delta E_{\text{orb}}(a'')$  interaction energy comes from  $\text{H}_3\text{B}-\text{L}$   $\pi_{\perp}$  donation and how much comes from  $\text{H}_3\text{B}-\text{L}$   $\pi_{\perp}$  backdonation. To address the question of  $\pi$ -donor strength of  $\text{CO}$  and  $\text{EC}_5\text{H}_5$ , and also to understand the differences in the nature of the chemical bond, we carried out EDA calculations on the complexes  $\text{H}_2\text{B}^+-\text{CO}$  and  $\text{H}_2\text{B}^+-\text{EC}_5\text{H}_5$ . The results are listed in Table 3.

The EDA calculations show that the  $\text{H}_2\text{B}^+-\text{L}$  bonds have more pronounced covalent character than the  $\text{H}_3\text{B}-\text{L}$  bonds. The relative contribution of the  $\Delta E_{\text{orb}}$  term to the attractive interactions in the former compounds is between 57.4 and 90.4% (Table 3), while it is only between 50.5 and 66.8% in the latter species. This can be explained by the much lower lying acceptor orbitals of the Lewis acid  $\text{BH}_2^+$  compared with the vacant orbitals of  $\text{BH}_3$ .<sup>[30]</sup> The EDA of the  $\text{H}_2\text{B}^+-\text{L}$  bonds could be carried out with  $C_{2v}$  symmetry, which makes it possible to separate the contributions of the in-plane  $\pi_{\parallel}$  orbitals ( $b_2$ ) from the out-of-plane  $\pi_{\perp}$  orbitals ( $b_1$ ) and from the  $\sigma$  orbitals ( $a_1$ ). The contributions of the  $a_2$  orbitals, which have  $\delta$  symmetry, arise from the admixture of the polarization functions. The calculated energy values of the latter are very small and can be neglected.

The calculated data for the  $\pi$ -orbital contribution to the  $\Delta E_{\text{orb}}$  term for  $\text{H}_2\text{B}^+-\text{L}$  indicate that the relative contribution of the in-plane  $\pi_{\parallel}$  orbitals ( $b_2$ ) is only between 1.9 and 6.4% for  $\text{L}=\text{EC}_5\text{H}_5$ , while it becomes 9.4% for  $\text{L}=\text{CO}$  (Table 3). The interaction of the  $\pi_{\parallel}$  orbitals arises from donation and backdonation between the Lewis acid and Lewis

Table 3. EDA results [ $\text{kcal mol}^{-1}$ ] for  $\text{H}_2\text{B}^+-\text{CO}$  and  $\text{H}_2\text{B}^+-\text{EC}_5\text{H}_5$  ( $\text{E}=\text{N}, \text{P}, \text{As}, \text{Sb}, \text{Bi}$ ) in  $C_{2v}$  symmetry and partial charges  $q(\text{BH}_2)$  at the BP86/TZ2P level.

Term	CO	N	P	As	Sb	Bi
$\Delta E_{\text{int}}$	-70.4	-146.2	-120.9	-107.3	-96.9	-82.7
$\Delta E_{\text{Pauli}}$	110.4	151.5	117.7	98.0	81.8	67.7
$\Delta E_{\text{elstat}}^{[a]}$	-57.0 (31.5%)	-126.8 (42.6%)	-67.7 (28.4%)	-46.6 (22.7%)	-30.0 (16.8%)	-14.4 (9.6%)
$\Delta E_{\text{orb}}^{[a]}$	-123.7 (68.5%)	-170.8 (57.4%)	-170.9 (71.6%)	-158.6 (77.3%)	-148.1 (83.2%)	-136.0 (90.4%)
$a_1(\sigma)^{[b]}$	-103.6 (83.8%)	-120.4 (70.5%)	-129.8 (76.0%)	-120.0 (75.7%)	-113.5 (76.4%)	-100.9 (74.2%)
$a_2(\delta)^{[b]}$	0.0 (0.0%)	-3.4 (2.0%)	-1.6 (1.0%)	-1.2 (0.8%)	-1.0 (0.6%)	-0.8 (0.6%)
$b_1(\pi_{\perp})^{[b]}$	-8.5 (6.8%)	-36.1 (21.1%)	-32.1 (18.8%)	-32.0 (20.2%)	-30.4 (20.5%)	-31.7 (23.3%)
$b_2(\pi_{\parallel})^{[b]}$	-11.6 (9.4%)	-10.9 (6.4%)	-7.3 (4.3%)	-5.3 (3.3%)	-3.7 (2.5%)	-2.6 (1.9%)
$\Delta E_{\text{prep}}$	18.5	24.1	26.2	23.6	21.1	17.4
$D_e$	51.9	122.1	94.7	83.6	75.8	65.4
$D_o$	48.9	117.4	92.0	81.0	73.6	63.4
$q(\text{BH}_2)$	0.83	0.66	0.61	0.58	0.54	0.51

[a] The value in parentheses gives the percentage contribution to the total attractive interactions. [b] The value in parentheses gives the percentage contribution to the total orbital interactions.

Table 4. EDA results [kcal mol<sup>-1</sup>] for H<sub>2</sub>B<sup>+</sup>–CO with different C–B distances at the BP86/TZ2P level.

Term	C–B [Å]			
	1.45	1.508	1.55	1.611
$\Delta E_{\text{int}}$	-69.4	-71.3	-71.5	-70.4
$\Delta \Delta E_{\text{int}}^{[\text{c}]}$		-0.9		0.0
$\Delta E_{\text{Pauli}}$	165.9	143.3	128.9	110.3
$\Delta \Delta E_{\text{Pauli}}^{[\text{c}]}$		32.9		0.0
$\Delta E_{\text{elstat}}^{[\text{a}]}$	-72.3 (30.7 %)	-66.8 (31.1 %)	-62.8 (31.3 %)	-57.0 (31.5 %)
$\Delta \Delta E_{\text{elstat}}^{[\text{c}]}$		-9.8		0.0
$\Delta E_{\text{orb}}^{[\text{a}]}$	-163.0 (69.3 %)	-147.8 (68.9 %)	-137.6 (68.7 %)	-123.7 (68.5 %)
$\Delta \Delta E_{\text{orb}}^{[\text{c}]}$		-24.1		0.0
$a_1 (\sigma)^{[\text{b}]}$	-129.7 (79.6 %)	-120.2 (81.3 %)	-113.4 (82.4 %)	-103.6 (83.8 %)
$\Delta a_1 (\sigma)^{[\text{c}]}$		-16.6		0.0
$a_2 (\delta)^{[\text{b}]}$	0.0 (0.0 %)	0.0 (0.0 %)	0.0 (0.0 %)	0.0 (0.0 %)
$b_1 (\pi_{\perp})^{[\text{b}]}$	-13.5 (8.3 %)	-11.4 (7.7 %)	-10.0 (7.3 %)	-8.5 (6.8 %)
$b_2 (\pi_{\parallel})^{[\text{b}]}$	-19.7 (12.1 %)	-16.3 (11.0 %)	-14.2 (10.3 %)	-11.6 (9.4 %)
$\Delta b (\pi)^{[\text{d}]}$		-7.6		0.0
$\Delta E_{\text{prep}}$	23.3	21.5	20.3	18.5
$\Delta \Delta E_{\text{prep}}^{[\text{c}]}$		3.0		0.0
$D_e$	46.1	49.8	51.2	51.9
$\Delta D_e^{[\text{c}]}$		-2.1		0.0
$D_o$				48.9
$\Delta E_{\text{rel}}$	5.8	2.1	0.7	0.0

[a] The value in parentheses gives the percentage contribution to the total attractive interactions. [b] The value in parentheses gives the percentage contribution to the total orbital interactions. [c] Difference between the values at the equilibrium bond lengths of H<sub>2</sub>B<sup>+</sup>–CO and H<sub>3</sub>B–CO. [d] Difference between the  $\pi$ -orbital interactions ( $b_1 + b_2$ ) at the equilibrium bond lengths of H<sub>2</sub>B<sup>+</sup>–CO and H<sub>3</sub>B–CO.

base. The orbital interaction of the out-of-plane  $\pi_{\perp}$  orbitals ( $b_1$ ) in H<sub>2</sub>B<sup>+</sup>–L comes only from H<sub>2</sub>B<sup>+</sup>←L donation, because BH<sub>2</sub><sup>+</sup> does not have an occupied  $\pi_{\perp}$  orbital. The data for the  $\Delta E_{\text{orb}}(b_1)$  contribution in H<sub>2</sub>B<sup>+</sup>–L are thus a direct measure of the  $\pi_{\perp}$  donor strength of L. Table 4 shows that the  $\pi$ -donor strength of CO is rather small, only 8.5 kcal mol<sup>-1</sup>, which contributes 6.8% to the  $\Delta E_{\text{orb}}$  term. The  $\pi_{\perp}$  donor strength of the heterobenzene ligands EC<sub>5</sub>H<sub>5</sub> is significantly higher. The  $\Delta E_{\text{orb}}(b_1)$  contribution to the  $\Delta E_{\text{orb}}$  term is remarkably constant between 30.4 (E=Sb) and 36.1 kcal mol<sup>-1</sup> (E=N). The relative contributions of  $\pi_{\parallel}$  donation are between 18.8 (E=P) and 23.3% (E=Bi). The EDA results clearly demonstrate that the heterobenzene ligands EC<sub>5</sub>H<sub>5</sub> are mainly  $\sigma$ -donor ligands, but the  $\pi_{\perp}$  donor strength is not negligible. The  $\pi_{\perp}$  donation of EC<sub>5</sub>H<sub>5</sub> in a donor–acceptor complex may contribute about 20% to the total orbital interactions if the Lewis acid has a low-lying empty  $\pi_{\perp}$  orbital.

The next part of the bonding analysis focuses on why the H<sub>2</sub>B<sup>+</sup>–CO bond is stronger but longer than the H<sub>3</sub>B–CO bond, and why the heterobenzene ligands EC<sub>5</sub>H<sub>5</sub> become much more strongly bonded than CO in H<sub>2</sub>B<sup>+</sup>–L whereas EC<sub>5</sub>H<sub>5</sub> is more weakly bonded than CO in the neutral complexes H<sub>3</sub>B–L. For the second question we compare the EDA results of H<sub>3</sub>B–EC<sub>5</sub>H<sub>5</sub> (Table 2) with the data for H<sub>2</sub>B<sup>+</sup>–EC<sub>5</sub>H<sub>5</sub> (Table 3). It becomes clear that the cations have a larger relative contribution of the  $\Delta E_{\text{orb}}$  term to the attractive B–E interactions, which becomes between 57.4% for E=N and 90.4% for E=Bi. A striking difference between the  $\Delta E_{\text{orb}}$  values of the two sets of compounds is the significantly larger contribution of the  $\pi_{\perp}$  orbitals in H<sub>2</sub>B<sup>+</sup>–

EC<sub>5</sub>H<sub>5</sub>, which accounts for an increase of of the interaction energy by about 30 kcal mol<sup>-1</sup>. An even larger increase on going from H<sub>3</sub>B–EC<sub>5</sub>H<sub>5</sub> to H<sub>2</sub>B<sup>+</sup>–EC<sub>5</sub>H<sub>5</sub> is calculated for the  $\sigma + \pi_{\parallel}$  orbitals, which contribute 55–70 kcal mol<sup>-1</sup> more to the orbital interaction of the latter complexes (Tables 2 and 3). The increase in the in-plane orbital interactions ( $\sigma + \pi_{\parallel}$ ) is partly compensated by the increased Pauli repulsion, which also becomes larger (6–30 kcal mol<sup>-1</sup>). Interestingly, the  $\Delta E_{\text{Pauli}}$  value of H<sub>2</sub>B<sup>+</sup>–PC<sub>5</sub>H<sub>5</sub> is only 6.0 kcal mol<sup>-1</sup> larger than that of H<sub>3</sub>B–PC<sub>5</sub>H<sub>5</sub>.

The strength of the electrostatic interactions changes only slightly (<10 kcal mol<sup>-1</sup>) between H<sub>3</sub>B–EC<sub>5</sub>H<sub>5</sub> and H<sub>2</sub>B<sup>+</sup>–EC<sub>5</sub>H<sub>5</sub> except for E=N, for which the  $\Delta E_{\text{elstat}}$  term increases by 40.3 kcal mol<sup>-1</sup>. This explains

why H<sub>2</sub>B<sup>+</sup>–NC<sub>5</sub>H<sub>5</sub> clearly has the strongest donor–acceptor bond of all compounds investigated here. The absolute and relative contributions of  $\Delta E_{\text{elstat}}$  to the donor–acceptor bonding in the heavier H<sub>2</sub>B<sup>+</sup>–EC<sub>5</sub>H<sub>5</sub> species become significantly smaller than for E=N (Table 3).

In summary, the much larger interaction energies in H<sub>2</sub>B<sup>+</sup>–EC<sub>5</sub>H<sub>5</sub> compared with H<sub>3</sub>B–EC<sub>5</sub>H<sub>5</sub> are caused by several factors. One factor is the significantly larger contribution of the  $\pi_{\perp}$  orbitals in H<sub>2</sub>B<sup>+</sup>–EC<sub>5</sub>H<sub>5</sub>, which accounts for an increase of about 30 kcal mol<sup>-1</sup> in the interaction energy. A second important factor is the increased binding interactions of the  $\sigma + \pi_{\parallel}$  orbitals, which strengthen the donor–acceptor bonds of the cations by 55–70 kcal mol<sup>-1</sup>. The increased Pauli repulsion between electrons having the same spin in the  $\sigma + \pi_{\parallel}$  orbitals reduces the net binding effect in H<sub>2</sub>B<sup>+</sup>–EC<sub>5</sub>H<sub>5</sub> by up to 30 kcal mol<sup>-1</sup>. The contribution of the electrostatic interactions to the enhanced binding is less than 10 kcal mol<sup>-1</sup> except for E=N, for which the  $\Delta E_{\text{elstat}}$  term increases by 40.3 kcal mol<sup>-1</sup>.

To explain the longer but stronger H<sub>2</sub>B<sup>+</sup>–CO bond compared with H<sub>3</sub>B–CO, we performed EDA calculations on molecules with different B–C bond lengths. The numerical results are given in Tables 4 and 5.

The geometries of H<sub>2</sub>B<sup>+</sup>–CO and H<sub>3</sub>B–CO were optimized with frozen B–C distances of 1.45, 1.508 (equilibrium distance of H<sub>3</sub>B–CO), 1.55, and 1.611 Å (equilibrium distance of H<sub>2</sub>B<sup>+</sup>–CO). Tables 4 and 5 show that the energy differences between the equilibrium structures and the species which are calculated with the optimized B–C bond length of the other species are rather small. It takes only 2.1 kcal mol<sup>-1</sup> to contract the H<sub>2</sub>B<sup>+</sup>–CO bond to the value

Table 5. EDA results [kcal mol<sup>-1</sup>] for H<sub>3</sub>B–CO with different C–B distances at the BP86/TZ2P level.

Term	C–B [Å]			
	1.45	1.508	1.55	1.611
$\Delta E_{\text{int}}$	-50.2	-50.3	-49.2	-45.5
$\Delta\Delta E_{\text{int}}^{[\text{c}]}$		-4.8		0.0
$\Delta E_{\text{Pauli}}$	177.5	151.9	135.9	117.1
$\Delta\Delta E_{\text{Pauli}}^{[\text{c}]}$		34.8		0.0
$\Delta E_{\text{elstat}}^{[\text{a}]}$	-82.4 (36.2 %)	-73.9 (36.5 %)	-68.1 (36.8 %)	-60.7 (37.3 %)
$\Delta\Delta E_{\text{elstat}}^{[\text{c}]}$		-13.2		0.0
$\Delta E_{\text{orb}}^{[\text{a}]}$	-145.2 (63.8 %)	-128.3 (63.5 %)	-117.0 (63.2 %)	-101.9 (62.7 %)
$\Delta\Delta E_{\text{orb}}^{[\text{c}]}$		-26.4		0.0
$a_1(\sigma)^{[\text{b}]}$	-101.1 (69.6 %)	-91.1 (71.0 %)	-84.1 (71.9 %)	-74.6 (73.2 %)
$\Delta a_1(\sigma)^{[\text{c}]}$		-16.5		0.0
$e(\pi)^{[\text{b}]}$	-44.1 (30.4 %)	-37.2 (29.0 %)	-32.9 (28.1 %)	-27.3 (26.8 %)
$\Delta e(\pi)^{[\text{c}]}$		-9.9		0.0
$\Delta E_{\text{prep}}$	14.0	13.2	12.6	10.6
$\Delta\Delta E_{\text{prep}}^{[\text{c}]}$		2.6		0.0
$D_e$	36.2	37.1	36.6	34.9
$\Delta D_e^{[\text{c}]}$		2.2		0.0
$D_o$		33.9		
$\Delta E_{\text{rel}}$	0.9	0.0	0.5	2.2

[a] The value in parentheses gives the percentage contribution to the total attractive interactions. [b] The value in parentheses gives the percentage contribution to the total orbital interactions. [c] Difference between the values at the equilibrium bond lengths of H<sub>2</sub>B<sup>+</sup>–CO and H<sub>3</sub>B–CO.

in H<sub>3</sub>B–CO, and only 2.2 kcal mol<sup>-1</sup> is necessary to stretch the H<sub>3</sub>B–CO bond to the value in H<sub>2</sub>B<sup>+</sup>–CO.

The EDA data (Tables 2–4) show that the interaction energy of H<sub>2</sub>B<sup>+</sup>–CO ( $\Delta E_{\text{int}} = -70.4$  kcal mol<sup>-1</sup>) is higher than that of H<sub>3</sub>B–CO ( $\Delta E_{\text{int}} = -50.3$  kcal mol<sup>-1</sup>), but the three major components  $\Delta E_{\text{elstat}}$ ,  $\Delta E_{\text{Pauli}}$ , and  $\Delta E_{\text{orb}}$  are weaker in the cation than in the neutral system, which is reasonable because of the longer donor–acceptor bond in H<sub>2</sub>B<sup>+</sup>–CO. The most striking result is that the value of  $\Delta E_{\text{int}}$  in H<sub>2</sub>B<sup>+</sup>–CO becomes larger when the B–C bond is shortened (Table 4). This means that the equilibrium bond length in H<sub>2</sub>B<sup>+</sup>–CO is not the distance at which the net attractive donor–acceptor interactions are strongest. Table 4 shows that the  $\Delta E_{\text{int}}$  values at 1.55 Å ( $-71.5$  kcal mol<sup>-1</sup>) and even at 1.508 Å ( $-71.3$  kcal mol<sup>-1</sup>) are larger than the equilibrium value at 1.611 Å ( $-70.4$  kcal mol<sup>-1</sup>). The reason why the total energy of H<sub>2</sub>B<sup>+</sup>–CO is lower at the longer distance lies in the lower preparation energy  $\Delta E_{\text{prep}}$  of the fragments (Table 4). The stronger interaction energy of H<sub>2</sub>B<sup>+</sup>–CO at shorter distances is compensated by the deformation energy of the fragments H<sub>2</sub>B<sup>+</sup> and CO. Inspection of the energy values reveals that the major contribution to  $\Delta E_{\text{prep}}$  comes from the bending deformation of H<sub>2</sub>B<sup>+</sup>.

So what is the difference between H<sub>2</sub>B<sup>+</sup>–CO and H<sub>3</sub>B–CO which explains the peculiar bond length/bond strength correlation? We compare the changes in the energy terms of the EDA calculated at the equilibrium values of H<sub>2</sub>B<sup>+</sup>–CO (1.611 Å) and H<sub>3</sub>B–CO (1.508 Å). At the shorter bond length, the  $\Delta E_{\text{prep}}$  value for H<sub>2</sub>B<sup>+</sup>–CO increases by 3.0 kcal mol<sup>-1</sup>, while that of H<sub>3</sub>B–CO increases by only 2.6 kcal mol<sup>-1</sup> (Tables 4 and 5). Thus, the  $\Delta E_{\text{prep}}$  values favor the neutral species at the short bond length of 1.508 Å by only 0.4 kcal mol<sup>-1</sup>. A much larger difference is found when the interaction energies are compared. The  $\Delta E_{\text{int}}$  value for H<sub>2</sub>B<sup>+</sup>–CO at the shorter bond length is only 0.9 kcal mol<sup>-1</sup>

higher than at its equilibrium value, while the  $\Delta E_{\text{int}}$  value for H<sub>3</sub>B–CO becomes 4.8 kcal mol<sup>-1</sup> larger when the bond length becomes shorter. The difference between the two species is 3.9 kcal mol<sup>-1</sup>. The main difference between the two energy terms of H<sub>2</sub>B<sup>+</sup>–CO and H<sub>3</sub>B–CO which give the dissociation energy thus come from the  $\Delta E_{\text{int}}$  values but not from the  $\Delta E_{\text{prep}}$  values. The breakdown of the  $\Delta E_{\text{int}}$  values of the two compounds shows (Tables 4 and 5) that the increase in Pauli repulsion in H<sub>3</sub>B–CO at shorter distance is larger (34.8 kcal mol<sup>-1</sup>) than in H<sub>2</sub>B<sup>+</sup>–CO (33.0 kcal mol<sup>-1</sup>). The difference is 1.8 kcal mol<sup>-1</sup>. The stronger increase of the

$\Delta E_{\text{int}}$  value in the neutral compound at shorter distance by 3.9 kcal mol<sup>-1</sup> must therefore come from an increase in the attractive interactions. The EDA data in Tables 4 and 5 show that 3.4 kcal mol<sup>-1</sup> comes from the increase in  $\Delta E_{\text{elstat}}$ , while 2.3 kcal mol<sup>-1</sup> originates from stronger orbital interactions. The total increase in attractive interactions by 5.7 kcal mol<sup>-1</sup> becomes smaller by 1.8 kcal mol<sup>-1</sup> larger Pauli repulsion yielding a 3.9 kcal mol<sup>-1</sup> larger  $\Delta\Delta E_{\text{int}}$  value for H<sub>3</sub>B–CO. Note that the larger increase of the orbital interactions  $\Delta\Delta E_{\text{orb}}$  in the neutral compound comes exclusively from the  $\pi$  interactions, which become stronger by 9.9 kcal mol<sup>-1</sup>, whereas in the cation the  $\Delta(\pi)$  value increases only by 7.6 kcal mol<sup>-1</sup>.

Closer examination of the trend of the energy terms of H<sub>2</sub>B<sup>+</sup>–CO and H<sub>3</sub>B–CO reveals interesting details about the differences in the bonding interactions. At the shorter equilibrium distance of H<sub>3</sub>B–CO (1.508 Å) the interaction energy in H<sub>2</sub>B<sup>+</sup>–CO ( $\Delta E_{\text{int}} = -71.3$  kcal mol<sup>-1</sup>) is still much higher than in H<sub>3</sub>B–CO ( $\Delta E_{\text{int}} = -50.3$  kcal mol<sup>-1</sup>), because in the former the Pauli repulsion is weaker ( $\Delta E_{\text{Pauli}} = 143.3$  kcal mol<sup>-1</sup>) and the orbital interaction is much stronger ( $\Delta E_{\text{orb}} = -147.8$  kcal mol<sup>-1</sup>) than in the latter ( $\Delta E_{\text{Pauli}} = 151.9$  kcal mol<sup>-1</sup>;  $\Delta E_{\text{orb}} = -128.3$  kcal mol<sup>-1</sup>). The larger Pauli repulsion comes from the additional B–H electron pair in H<sub>3</sub>B–CO, while the larger  $\Delta E_{\text{orb}}$  value comes mainly from the  $\sigma$ -orbital interactions (Table 4), which are caused by the low-lying empty  $\sigma$  orbital in BH<sub>2</sub><sup>+</sup>. However, the electrostatic attraction in H<sub>2</sub>B<sup>+</sup>–CO at  $d(\text{B–C}) = 1.508$  Å ( $\Delta E_{\text{elstat}} = -66.8$  kcal mol<sup>-1</sup>) is weaker than in H<sub>3</sub>B–CO ( $\Delta E_{\text{elstat}} = -73.9$  kcal mol<sup>-1</sup>). Like the larger Pauli repulsion, this comes from the additional B–H electron pair. In summary, the longer but stronger bond in H<sub>2</sub>B<sup>+</sup>–CO compared with H<sub>3</sub>B–CO is mainly due to the change in the electrostatic attraction and  $\pi$  bonding at shorter distances and to a lesser extent to the deformation energy of the fragments.

What difference between the Lewis bases CO and EC<sub>5</sub>H<sub>5</sub> causes the different behavior in the interactions with the Lewis acids BH<sub>3</sub> and BH<sub>2</sub><sup>+</sup>? Heteroarenes like CO bind more strongly to the cation BH<sub>2</sub><sup>+</sup> than to neutral BH<sub>3</sub>, but the donor–acceptor bond becomes shorter in the former complexes and the increase in the bond strength is much larger (Table 1). Since this behavior is found for all heteroarenes EC<sub>5</sub>H<sub>5</sub> (E=N–Bi) and because the preparation energy plays only a minor role (see Table 1) we analyzed only the interaction energies of the nitrogen systems H<sub>2</sub>B<sup>+</sup>–NC<sub>5</sub>H<sub>5</sub> and H<sub>3</sub>B–NC<sub>5</sub>H<sub>5</sub> at different B–N bond lengths. The results are listed in Tables 6 and 7.

A comparison of the  $\Delta E_{\text{int}}$  values of the two systems at their equilibrium distances of 1.605 (H<sub>3</sub>B–NC<sub>5</sub>H<sub>5</sub>) and 1.491 Å (H<sub>2</sub>B<sup>+</sup>–NC<sub>5</sub>H<sub>5</sub>) shows that bond shortening yields a greater increase in binding energy in H<sub>2</sub>B<sup>+</sup>–NC<sub>5</sub>H<sub>5</sub> (–6.1 kcal mol<sup>–1</sup>) than in H<sub>3</sub>B–NC<sub>5</sub>H<sub>5</sub> (–2.0 kcal mol<sup>–1</sup>). This is opposite to the CO complexes, where the neutral complex H<sub>3</sub>B–CO exhibited a larger increase of  $\Delta E_{\text{int}}$  at shorter distance than the charged species H<sub>2</sub>B<sup>+</sup>–CO. Part of the larger increase in  $\Delta E_{\text{int}}$  value in H<sub>2</sub>B<sup>+</sup>–NC<sub>5</sub>H<sub>5</sub> comes from the Pauli term, which increase by 2.0 kcal mol<sup>–1</sup> less than in H<sub>3</sub>B–NC<sub>5</sub>H<sub>5</sub> (Tables 6 and 7). The remainder comes from the orbital interactions, which increase more in H<sub>2</sub>B<sup>+</sup>–NC<sub>5</sub>H<sub>5</sub> than in H<sub>3</sub>B–NC<sub>5</sub>H<sub>5</sub> by 3.1 kcal mol<sup>–1</sup>, while the latter system actually enjoys a larger increase of the electrostatic attraction at shorter distance than the former complex. The large increase of the  $\Delta E_{\text{orb}}$  term particularly benefits from the significantly stronger  $\pi_{\perp}$  interactions in H<sub>2</sub>B<sup>+</sup>–NC<sub>5</sub>H<sub>5</sub>, which show an absolute increase by –8.4 kcal mol<sup>–1</sup> and a relative increase from 19.0 to 21.1%. This clearly indicates that H<sub>2</sub>B<sup>+</sup>–NC<sub>5</sub>H<sub>5</sub>  $\pi_{\perp}$  donation plays an important role in binding.

The above discussion shows that the ligands CO and EC<sub>5</sub>H<sub>5</sub> exhibit a different behavior concerning  $\pi$ -orbital interactions. CO is a clearly stronger  $\pi$  acceptor but weaker  $\pi$  donor than EC<sub>5</sub>H<sub>5</sub>. The latter can easily be explained with the energy levels of the highest occupied  $\pi$  orbitals. The occupied

$\pi$  orbital of CO is energetically much lower lying (–11.84 eV) than the highest occupied  $\pi$  orbitals of EC<sub>5</sub>H<sub>5</sub>, which have a coefficient at atom E ( $b_1$  symmetry). The energy levels of the latter are between –5.28 (E=Bi) and –7.33 eV (E=N).<sup>[5a]</sup> The greater  $\pi$ -acceptor strength of CO can not easily be explained with the orbital energy. The  $b_1(\pi)$  LUMO of CO (–2.08 eV) is lower lying than the  $b_1(\pi)$  LUMO of NC<sub>5</sub>H<sub>5</sub> (–1.91 eV) but it is higher in energy than the  $b_1(\pi)$  LUMO of the other EC<sub>5</sub>H<sub>5</sub> molecules, which lie between –2.40 (E=P) and –2.78 eV (E=Sb). The much longer H<sub>2</sub>B<sup>+</sup>–EC<sub>5</sub>H<sub>5</sub> and H<sub>3</sub>B–EC<sub>5</sub>H<sub>5</sub> distances for the heavier elements E yield smaller overlaps of the  $\pi$  orbitals which weaken the  $\pi$ -acceptor strength.

An interesting detail in the calculated data for H<sub>3</sub>B–CO and H<sub>2</sub>B<sup>+</sup>–CO deserves special attention. The calculated C–O distance in H<sub>2</sub>B<sup>+</sup>–CO is shorter than in H<sub>3</sub>B–CO. The theoretically predicted shortening at the BP86/TZ2P level is

Table 6. EDA results [kcal mol<sup>–1</sup>] for H<sub>2</sub>B<sup>+</sup>–NC<sub>5</sub>H<sub>5</sub> with different B–N distances at the BP86/TZ2P level.

Term	B–N [Å]			
	1.450	1.491	1.550	1.605
$\Delta E_{\text{int}}$	–146.8	–146.2	–143.6	–140.1
$\Delta\Delta E_{\text{int}}^{[c]}$		–6.1		0.0
$\Delta E_{\text{Pauli}}$	168.2	151.5	129.7	112.4
$\Delta\Delta E_{\text{Pauli}}^{[c]}$		39.1		0.0
$\Delta E_{\text{elstat}}^{[a]}$	–134.5 (42.7%)	–126.8 (42.6%)	–116.0 (42.4%)	–106.6 (42.2%)
$\Delta\Delta E_{\text{elstat}}^{[c]}$		–20.2		0.0
$\Delta E_{\text{orb}}^{[a]}$	–180.5 (57.3%)	–170.8 (57.4%)	–157.4 (57.6%)	–145.9 (57.8%)
$\Delta\Delta E_{\text{orb}}^{[c]}$		–24.9		0.0
$a_1(\sigma)^{[b]}$	–125.1 (69.3%)	–120.4 (70.5%)	–113.2 (71.9%)	–106.7 (73.2%)
$\Delta a_1(\sigma)^{[c]}$		–13.7		0.0
$a_2(\delta)^{[b]}$	–3.5 (1.9%)	–3.4 (2.0%)	–3.2 (2.0%)	–3.1 (2.1%)
$\Delta a_2(\delta)^{[c]}$		–0.3		0.0
$b_1(\pi_{\perp})^{[b]}$	–39.8 (22.1%)	–36.1 (21.1%)	–31.4 (20.0%)	–27.7 (19.0%)
$\Delta b_1(\pi_{\perp})^{[c]}$		–8.4		0.0
$b_2(\pi_{\parallel})^{[b]}$	–12.1 (6.7%)	–10.9 (6.4%)	–9.5 (6.1%)	–8.4 (5.8%)
$\Delta b_2(\pi_{\parallel})^{[c]}$		–2.5		0.0

[a] The value in parentheses gives the percentage contribution to the total attractive interactions. [b] The value in parentheses gives the percentage contribution to the total orbital interactions. [c] Difference between the values at the equilibrium bond lengths of H<sub>2</sub>B<sup>+</sup>–NC<sub>5</sub>H<sub>5</sub> and H<sub>3</sub>B–NC<sub>5</sub>H<sub>5</sub>.

Table 7. EDA results [kcal mol<sup>–1</sup>] for H<sub>3</sub>B–NC<sub>5</sub>H<sub>5</sub> with different B–N distances at the BP86/TZ2P level.

Term	B–N [Å]			
	1.450	1.491	1.550	1.605
$\Delta E_{\text{int}}$	–52.4	–53.1	–52.6	–51.1
$\Delta\Delta E_{\text{int}}^{[c]}$		–2.0		0.0
$\Delta E_{\text{Pauli}}$	180.9	163.1	140.5	122.0
$\Delta\Delta E_{\text{Pauli}}^{[c]}$		41.1		0.0
$\Delta E_{\text{elstat}}^{[a]}$	–116.0 (49.7%)	–107.7 (49.8%)	–96.4 (49.9%)	–86.5 (49.9%)
$\Delta\Delta E_{\text{elstat}}^{[c]}$		–21.2		0.0
$\Delta E_{\text{orb}}^{[a]}$	–117.3 (50.3%)	–108.5 (50.2%)	–96.7 (50.1%)	–86.7 (50.1%)
$\Delta\Delta E_{\text{orb}}^{[c]}$		–21.8		0.0
$a'(\sigma+\pi_{\parallel})^{[b]}$	–101.1 (86.2%)	–94.6 (87.2%)	–85.7 (88.6%)	–77.7 (89.6%)
$\Delta a'(\sigma+\pi_{\parallel})^{[c]}$		–16.9		0.0
$a''(\pi_{\perp})^{[b]}$	–16.2 (13.8%)	–13.8 (12.8%)	–11.1 (11.5%)	–9.0 (10.4%)
$\Delta a''(\pi_{\perp})^{[c]}$		–4.8		0.0

[a] The value in parentheses gives the percentage contribution to the total attractive interactions. [b] The symmetry notation in parentheses refers to the orbitals of the donor moiety. The value in parentheses gives the percentage contribution to the total orbital interactions. [c] The symmetry notation in parentheses refers to the orbitals of the donor moiety. The values give the difference between the results at the equilibrium bond lengths of H<sub>2</sub>B<sup>+</sup>–NC<sub>5</sub>H<sub>5</sub> and H<sub>3</sub>B–NC<sub>5</sub>H<sub>5</sub>.



0.021 Å, while the difference at the QCISD(T)/6-311G(d,p) level is 0.019 Å (Table 1). Both methods predict that the C–O bond lengths in  $\text{H}_2\text{B}^+\text{--CO}$  are also shorter than in free CO by 0.014 Å (BP86/TZ2P) and 0.016 Å (QCISD(T)/6-311G(d,p)). Carbonyl complexes which have shorter C–O distances than CO have been termed nonclassical carbonyls.<sup>[31]</sup> The shortening indicates that  $\text{H}_2\text{B}^+\text{--CO}$   $\pi$  backdonation should be very small, since the donation into the  $\pi^*$  orbital of CO yields a longer bond. Theoretical studies have shown that the strength of  $\text{M--CO}$   $\pi$  backdonation, where M is a transition metal, correlates well with the lengthening of the C–O bond.<sup>[32]</sup> The strength of  $\text{H}_2\text{B}^+\text{--CO}$   $\pi$  backdonation can be quantitatively estimated from the EDA results in Table 3. The  $b_1$  contribution of the  $\Delta E_{\text{orb}}$  term ( $-8.5$  kcal mol<sup>-1</sup>) gives the  $\pi_{\perp}$  interactions, which only come from  $\text{H}_2\text{B}^+\text{--CO}$  donation. The  $b_2$  contribution gives the  $\pi_{\parallel}$  interactions ( $-11.6$  kcal mol<sup>-1</sup>). Since the in-plane and out-of-plane  $\pi$  orbitals of CO are degenerate, the difference between the  $b_1$  and  $b_2$  values directly gives the strength of  $\text{H}_2\text{B}^+\text{--CO}$   $\pi$  backdonation, which is only  $-3.1$  kcal mol<sup>-1</sup>. The strength of the  $\pi$  interactions in  $\text{H}_3\text{B--CO}$  is  $-37.2$  kcal mol<sup>-1</sup> (Table 2, twice the value of the  $\pi_{\perp}$  interactions). To estimate the contribution of the  $\text{H}_3\text{B--CO}$   $\pi$  backdonation to this value, we carried out EDA calculations on  $\text{H}_3\text{B--CO}$  in which the vacant  $\pi^*$  orbitals of CO were deleted. The calculated value for the remaining  $\pi$  interactions is only  $-5.6$  kcal mol<sup>-1</sup>. The difference between this value and the total  $\pi$  interactions ( $-37.2$  kcal mol<sup>-1</sup>) is  $-31.6$  kcal mol<sup>-1</sup>, which gives the strength of  $\text{H}_3\text{B--CO}$   $\pi$  backdonation. The last-named value is significantly larger than the calculated  $\text{H}_2\text{B}^+\text{--CO}$   $\pi$  backdonation of  $-3.1$  kcal mol<sup>-1</sup>.

The significant contribution of the  $\text{H}_3\text{B--CO}$   $\pi$  backdonation to the orbital interactions is in agreement with the calculated partial charges (Table 2), which suggest that the Lewis acid  $\text{BH}_3$  carries a small positive charge in  $\text{H}_3\text{B--CO}$ , while it has a small negative charge in  $\text{H}_3\text{B--EC}_5\text{H}_5$ . The same trend is also found in  $\text{H}_2\text{B}^+\text{--L}$ , in which the charge donation from  $\text{L=CO}$  to the  $\text{BH}_2^+$  fragment is only 0.17e, while for  $\text{L=EC}_5\text{H}_5$  it is in the range 0.34–0.49e (Table 3).

What causes the C–O bond in  $\text{H}_2\text{B}^+\text{--CO}$  to become shorter than in free CO? The orbital interactions in  $\text{H}_2\text{B}^+\text{--CO}$  are dominated by the  $\sigma$  orbitals (Table 3). A popular textbook explanation suggests that the  $\sigma$  HOMO of CO is antibonding, but the shape of the HOMO does not show a node between the atoms.<sup>[4,33]</sup> Detailed investigations of the factors which influence the C–O bonds revealed that a positive charge which approaches CO from the carbon end yields a shorter bond because the CO orbitals become less polarized towards oxygen.<sup>[34]</sup> This leads to a larger overlap of the atomic orbitals, and the MOs become more like those in  $\text{N}_2$ . This explanation is in agreement with the finding that the C–O bond becomes longer when a positive charge approaches CO from the oxygen end. An antibonding HOMO should lead to bond lengthening in both cases.

The above discussion about the bonding situation in the complexes demonstrates the detailed insight which can be gained from the results of EDA. The EDA calculations

make it possible to discuss the differences among the binding interactions in  $\text{H}_3\text{B--CO}$ ,  $\text{H}_3\text{B--EC}_5\text{H}_5$ ,  $\text{H}_2\text{B}^+\text{--CO}$ , and  $\text{H}_2\text{B}^+\text{--EC}_5\text{H}_5$  in terms of well-defined energy contributions which provide a quantitative estimate of the strength not only of  $\sigma$  and  $\pi$  orbital bonding, but also of electrostatic bonding and Pauli repulsion. The last-named contributions are often neglected in discussions of chemical bonding that focus only on orbital interactions.

## Conclusion

The calculated BDEs of the donor–acceptor complexes  $\text{H}_3\text{B--L}$  ( $\text{L=CO}$ ,  $\text{EC}_5\text{H}_5$ ) at the BP86/TZ2P level have values between  $D_e=37.1$  kcal mol<sup>-1</sup> for  $\text{H}_3\text{B--CO}$  and  $D_e=6.9$  kcal mol<sup>-1</sup> for  $\text{H}_3\text{B--BiC}_5\text{H}_5$ . The BDE trend is  $\text{CO} > \text{N} > \text{P} > \text{As} > \text{Sb} > \text{Bi}$ . The BDEs of the cations  $\text{H}_2\text{B}^+\text{--CO}$  and  $\text{H}_2\text{B}^+\text{--EC}_5\text{H}_5$  are larger, particularly for the complexes of the heterobenzene ligands. The calculated values are between  $D_e=51.9$  kcal mol<sup>-1</sup> for  $\text{H}_2\text{B}^+\text{--CO}$  and  $D_e=122.1$  kcal mol<sup>-1</sup> for  $\text{H}_2\text{B}^+\text{--NC}_5\text{H}_5$ . The BDE trend of  $\text{H}_2\text{B}^+\text{--CO}$  and  $\text{H}_2\text{B}^+\text{--EC}_5\text{H}_5$  is  $\text{N} > \text{P} > \text{As} > \text{Sb} > \text{Bi} > \text{CO}$ . The energy decomposition analysis of the donor–acceptor bonds shows that the contributions of the orbital interactions to the donor–acceptor binding are always larger than the electrostatic contributions, particularly for the bonds in the cations. The largest contributions to the orbital interactions come from the  $\sigma$  orbitals. The heterobenzene ligands may become moderately strong  $\pi$  donors in complexes with strong Lewis acids, while CO is only a weak  $\pi$  donor.

The much larger interaction energies in  $\text{H}_2\text{B}^+\text{--EC}_5\text{H}_5$  compared with  $\text{H}_3\text{B--EC}_5\text{H}_5$  are caused by the significantly larger contribution of the  $\pi_{\perp}$  orbitals in  $\text{H}_2\text{B}^+\text{--EC}_5\text{H}_5$  and by the increase of the binding interactions of the  $\sigma+\pi_{\parallel}$  orbitals. The contribution of the electrostatic interactions to the enhanced binding is small except for  $\text{E=N}$ , for which the  $\Delta E_{\text{elstat}}$  term increases by 40.3 kcal mol<sup>-1</sup>. The reason for the longer but stronger bond in  $\text{H}_2\text{B}^+\text{--CO}$  compared with that in  $\text{H}_3\text{B--CO}$  comes mainly from the change in the electrostatic attraction and the  $\pi$  bonding at shorter distances, which increases more in the neutral system than in the cation, and to a lesser extent from the deformation energy of the fragments.  $\text{H}_2\text{B}^+\text{--NC}_5\text{H}_5$   $\pi_{\perp}$  donation plays an important role for the stronger interactions at shorter distances compared with  $\text{H}_3\text{B--NC}_5\text{H}_5$ .

## Acknowledgements

We thank one referee whose constructive comments helped to improve the manuscript. The work was supported by the Deutsche Forschungsgemeinschaft. Excellent service by the Hochschulrechenzentrum of the Philipps-Universität Marburg is gratefully acknowledged. Additional computer time was provided by the HLRS Stuttgart and HHLRZ Darmstadt.

[1] M. J. S. Dewar, *Bull. Soc. Chim. Fr.* **1951**, 18, C79.

- [2] J. Chatt, L. A. Duncanson, *J. Chem. Soc.* **1953**, 2929.
- [3] a) G. Frenking, *J. Organomet. Chem.* **2001**, **635**, 9; b) G. Frenking in *Modern Coordination Chemistry: The Legacy of Joseph Chatt* (Eds.: G. J. Leigh, N. Winterton), The Royal Society, London, **2002**, p. 111.
- [4] The possibility of  $\pi$  donation from CO in carbonyl complexes was pointed out in C. Elschenbroich, A. Salzer, *Organometallics*, 2nd ed., VCH, Weinheim, **1992**, p. 227.
- [5] a) S. Erhardt, Ph. D. Thesis, Universität Marburg, **2005**; b) S. Erhardt, G. Frenking, unpublished results.
- [6] F. M. Bickelhaupt, E. J. Baerends, *Rev. Comput. Chem.*, Vol. 15 (Eds.: K. B. Lipkowitz, D. B. Boyd), Wiley-VCH, New York, **2000**, p. 1.
- [7] T. Ziegler, A. Rauk, *Theor. Chim. Acta* **1977**, **46**, 1.
- [8] a) K. Morokuma, *J. Chem. Phys.* **1971**, **55**, 1236; b) K. Kitaura, K. Morokuma, *Int. J. Quantum Chem.* **1976**, **10**, 325.
- [9] G. Frenking, K. Wichmann, N. Fröhlich, C. Loschen, M. Lein, J. Frunzke, V. M. Rayón, *Coord. Chem. Rev.* **2003**, **238–239**, 55.
- [10] R. G. Pearson, *Introduction to Hard and Soft Acids and Bases*, Dowden, Hutchinson, Ross, Stroudsburg, PA, **1973**.
- [11] a) R. J. Gillespie, I. Hargittai, *The VSEPR Model of Molecular Geometry*, Prentice-Hall, New Jersey, **1991**; b) R. J. Gillespie, P. L. A. Popelier, *Chemical Bonding and Molecular Geometry*, Oxford University Press, New York, **2001**, p. 191.
- [12] A. D. Becke, *Phys. Rev. A* **1988**, **38**, 3098.
- [13] J. P. Perdew, *Phys. Rev. B* **1986**, **33**, 8822.
- [14] J. G. Snijders, E. J. Baerends, P. Vernooijs, *At. Nucl. Data Tables* **1982**, **26**, 483.
- [15] J. Krijin, E. J. Baerends, *Fit Functions in the HFS-Method*, Internal Report (in Dutch), Vrije Universiteit Amsterdam, The Netherlands, **1984**.
- [16] a) C. Chang, M. Pelissier, Ph. Durand, *Phys. Scr.* **1986**, **34**, 394; b) J.-L. Heully, I. Lindgren, E. Lindroth, S. Lundquist, A.-M. Martensson-Pendrill, *J. Phys. B* **1986**, **19**, 2799; c) E. van Lenthe, E. J. Baerends, J. G. Snijders, *J. Chem. Phys.* **1993**, **99**, 4597; d) E. van Lenthe, E. J. Baerends, J. G. Snijders, *J. Chem. Phys.* **1996**, **105**, 6505; e) E. van Lenthe, R. van Leeuwen, E. J. Baerends, J. G. Snijders, *Int. J. Quantum Chem.* **1996**, **57**, 281.
- [17] E. L. Hirshfeld, *Theor. Chim. Acta* **1977**, **44**, 129.
- [18] G. te Velde, F. M. Bickelhaupt, E. J. Baerends, S. J. A. van Gisbergen, C. Fonseca Guerra, J. G. Snijders, T. Ziegler, *J. Comput. Chem.* **2001**, **22**, 931.
- [19] J. A. Pople, M. Head-Gordon, K. Raghavachari, *J. Chem. Phys.* **1987**, **87**, 5968.
- [20] R. Krishnan, J. S. Binkley, R. Seeger, J. A. Pople, *J. Chem. Phys.* **1980**, **72**, 650.
- [21] J. W. Ochterski, G. A. Petersson, J. A. Montgomery, *J. Chem. Phys.* **1996**, **104**, 2598.
- [22] Gaussian03, Revision C.02, M. J. Frisch, G. W. Trucks, H. B. Schlegel, G. E. Scuseria, M. A. Robb, J. R. Cheeseman, J. A. Montgomery, Jr., T. Vreven, K. N. Kudin, J. C. Burant, J. M. Millam, S. S. Iyengar, J. Tomasi, V. Barone, B. Mennucci, M. Cossi, G. Scalmani, N. Rega, G. A. Petersson, H. Nakatsuji, M. Hada, M. Ehara, K. Toyota, R. Fukuda, J. Hasegawa, M. Ishida, T. Nakajima, Y. Honda, O. Kitao, H. Nakai, M. Klene, X. Li, J. E. Knox, H. P. Hratchian, J. B. Cross, V. Bakken, C. Adamo, J. Jaramillo, R. Gomperts, R. E. Stratmann, O. Yazyev, A. J. Austin, R. Cammi, C. Pomelli, J. W. Ochterski, P. Y. Ayala, K. Morokuma, G. A. Voth, P. Salvador, J. J. Dannenberg, V. G. Zakrzewski, S. Dapprich, A. D. Daniels, M. C. Strain, O. Farkas, D. K. Malick, A. D. Rabuck, K. Raghavachari, J. B. Foresman, J. V. Ortiz, Q. Cui, A. G. Baboul, S. Clifford, J. Cioslowski, B. B. Stefanov, G. Liu, A. Liashenko, P. Piskorz, I. Komaromi, R. L. Martin, D. J. Fox, T. Keith, M. A. Al-Laham, C. Y. Peng, A. Nanayakkara, M. Challacombe, P. M. W. Gill, B. Johnson, W. Chen, M. W. Wong, C. Gonzalez, J. A. Pople, Gaussian, Inc., Wallingford, CT, **2004**.
- [23] A. C. Venkatachar, R. C. Taylor, R. L. Kuczkowski, *J. Mol. Struct.* **1977**, **38**, 17.
- [24] S. G. Lias, J. E. Bartmess, J. F. Liebman, J. L. Holmes, R. D. Levin, W. G. Mallard, *J. Phys. Chem. Ref. Data* **1988**, **17**, Suppl. 1.
- [25] V. Jonas, G. Frenking, M. T. Reetz, *J. Am. Chem. Soc.* **1994**, **116**, 8741.
- [26] P. R. Rablen, *J. Am. Chem. Soc.* **1997**, **119**, 8350.
- [27] a) C. Møller, M. S. Plesset, *Phys. Rev.* **1934**, **46**, 618; b) J. S. Binkley, J. A. Pople, *Int. J. Quantum Chem.* **1975**, **9S**, 229.
- [28] R. A. Fischer, M. M. Schulte, J. Weiss, L. Zsolnai, A. Jacobi, G. Huttner, G. Frenking, C. Boehme, S. F. Vyboishchikov, *J. Am. Chem. Soc.* **1998**, **120**, 1237.
- [29] D. Cremer, A. Wu, A. Larsson, E. Kraka, *J. Mol. Model.* **2000**, **6**, 396.
- [30] The contribution of the orbital term to the total interactions in H<sub>2</sub>B<sup>+</sup>–L is also enhanced by stronger polarization of the orbitals of L through positively charged BH<sub>2</sub><sup>+</sup>. The calculated partial charges indicate, however, that the charge transfer in H<sub>2</sub>B<sup>+</sup>–L is not much larger than in H<sub>3</sub>B–L. The  $\Delta q$  values in H<sub>2</sub>B<sup>+</sup>–EC<sub>3</sub>H<sub>3</sub> lie between 0.34e (E=N) and 0.49e (E=Bi). The  $\Delta q$  values in H<sub>3</sub>B–EC<sub>3</sub>H<sub>3</sub> are between 0.08e (E=P) and 0.14e (E=N).
- [31] a) S. H. Strauss, *Chemtracts: Inorg. Chem.* **1997**, **10**, 77; b) A. J. Lupinetti, G. Frenking, S. H. Strauss, *Angew. Chem.* **1998**, **110**, 2229; *Angew. Chem. Int. Ed.* **1998**, **37**, 2113; c) A. J. Lupinetti, S. H. Strauss, G. Frenking, *Prog. Inorg. Chem.* **2001**, **49**, 1.
- [32] a) A. W. Ehlers, S. Dapprich, S. F. Vyboishchikov, G. Frenking, *Organometallics* **1996**, **15**, 105; b) R. K. Szilagy, G. Frenking, *Organometallics* **1997**, **16**, 4807; c) A. J. Lupinetti, V. Jonas, W. Thiel, S. H. Strauss, G. Frenking, *Chem. Eur. J.* **1999**, **5**, 2573; d) A. Diefenbach, F. M. Bickelhaupt, G. Frenking, *J. Am. Chem. Soc.* **2000**, **122**, 6449.
- [33] T. A. Albright, J. K. Burdett, M. H. Whangbo, *Orbital Interactions in Chemistry*, Wiley, New York, **1985**, p. 82.
- [34] a) A. S. Goldman, K. Krogh-Jespersen, *J. Am. Chem. Soc.* **1996**, **118**, 12159; b) A. Lupinetti, S. Fau, G. Frenking, S. H. Strauss, *J. Phys. Chem. A* **1997**, **101**, 9551.

Received: May 25, 2005

Revised: February 1, 2006

Published online: April 6, 2006